Supporting Information

Habbe *et al.* 10.1073/pnas.0810097105

SI Text

SI Materials and Methods. ***Histology, immunohistochemistry, and immunofluorescence.*** Tissues were fixed in 10% neutral buffered formalin overnight, embedded in paraffin, and 4-μm serial sections prepared for histology with hematoxylin and eosin (H&E) stain, and for immunohistochemistry (IHC). For IHC, sections were deparaffinized in xylene and rehydrated in ethanol. Heat-induced epitope retrieval was accomplished in citrate buffer (pH 6.0) for 20 min in a Flavor Center Handy Steamer (Black&Decker). To block endogenous peroxidase activity, slides were incubated with 3% hydrogen peroxide for 10 min. The sections were then blocked at room temperature with TBS-T containing 10% FCS (20 nM Tris, 500 mM sodium chloride, and 0.05% Tween 20, pH 7.5) for 30 min. Primary antibodies were incubated at 4°C overnight. Thereafter, the LSAB+ kit (Dako) was used according to the manufacturer's recommendations, and visualization was performed using a DAB substrate kit (Vector). Hematoxylin counterstaining was performed, followed by dehydration in graded ethanol and xylene. Slides were mounted with Cytoseal60 permanent mounting media (Richard-Allan-Scientific). The primary antibodies used were: anti-proliferating cell nuclear antigen (PCNA) (DakoNovocastra, 1:100), anti-cytokeratin K19 (Developmental Studies Hybridoma Bank, 1:100), anti-amylase (Santa Cruz Biotechnology, 1:100), anti-Hes1 (a generous gift from Tetsuo Sudo, Pharmaceutical Research Laboratories; 1:2,000) and anti-Mist 1 (1:2,000), all of which have been previously described (1–4). For immunofluorescence analysis, tissues were fixed, sectioned and stained as described above. The following primary antibodies were used: anti-E-Cadherin (Zymed/Invitrogen, 1:200), anti-amylase (Santa Cruz Biotechnology, 1:500), and anti-Notch1 intra-cytoplasmic domain (N1-ICD) (Cell Signaling, 1:200), as previously described (3, 5). The secondary antibodies included biotin-conjugated anti-rat (1:500), anti-guinea pig (1:500) and anti-goat IgG (1:500) for regular IHC, and Cy3- or Cy2-conjugated streptavidin (1:1,000, 1:300), Cy3-conjugated anti-rabbit (1:300), and Cy5-conjugated anti-rat (1:300) for immunofluorescence. Visualization was performed with a confocal laser scanning microscope (410LSM, Zeiss) using a 40′ (NA 1.5) C-apochromat objective, and image analysis was performed using MetaMorph series 5.0 software (Universal Imaging).

Pancreata from *Mist1*$^{Cre\text{ERT2}/+}$; LSL-*Kras*$^{\text{G12D}}$; *Rosa*26R mice were processed for X-gal staining as follows: dissected pancreata were fixed in 4% paraformaldehyde for 1 h and incubated with 30% sucrose for 6–8 h at 4°C. After embedding in OCT (Sakura), 7 μm sections were obtained using a cryostat (Zeiss), stained with X-Gal for 5 h at 37°C and counterstained with nuclear fast red.

Microdissection and PCR for recombined the LSL-Kras^{G12D} allele in mPanIN lesions. Pancreatic tissues harvested from two *Ela-Cre*ERT2$^{\text{Tg}/+}$; LSL-*Kras*$^{\text{G12D}}$ mice at 12 months of age were embedded in Tissue-Tek OCT compound medium (Sakura), and snap-frozen in liquid nitrogen. The frozen samples were cut into 6 μm sections using a cryostat (Olympus) and embedded onto UV-treated PALM membrane slides (Carl Zeiss MicroImaging). Sections were fixed in cold methanol and stained with H&E before microdissection. Microdissection of five independent mPanIN lesions of different histological grades was performed using a PALM MicroBeam platform (Carl Zeiss MicroImaging). Genomic DNA from microdissected samples was extracted using QIAamp DNA MicroKit (QIAgen) according to the manufacturer's protocol. PCR primers for detecting the single *LoxP* site were as follows: 5′-GGG TAG GTG TTG GGA TAG CTG-3′ and 3′-TCC GAA TTC AGT GAC TAC AGA TGT ACA GAG. PCR was carried out using the REDExtract-N-Amp PCR ReadyMix (Sigma). PCR products were separated on a 2% agarose gel, yielding a 325-bp product (single LoxP site, successful recombination), or a 285-bp product (wild type-allele).

Results. ***Mist1 expression and Cre-mediated recombination in Mist1$^{CreERT2/+}$ mice is restricted to the differentiated acinar compartment and excludes centroacinar cells (CACs).*** In a recent study of mutant *Kras*-induced mPanINs in the mature pancreas, Guerra and colleagues were unable to exclude *Cre*-mediated recombination events in the CACs, based on the positive β-galactosidase expression observed in a fraction of these cells with their *Elastase* driver line on the Rosa26r background (6). The CACs likely harbor a distinct biology from that of terminally differentiated acinar cells, as evidenced by the persistence of Notch activation (7), and their putative role as a "stem cell" compartment in the adult pancreas (8). Therefore, it is imperative that recombination events occurring in the differentiated acinar compartment be distinguished from those happening in the CACs.

To circumvent this technical pitfall, we decided to use two independent strains, restricting *Cre* expression to either the *Elastase* (*Ela*) or the *Mist1* cellular domain, respectively. The particular *Ela-Cre*ERT2$^{\text{Tg}/+}$ line used in the current set of experiments has been previously described (9, 10), and lineage tracing studies using *Rosa26*R reporter mice have shown that recombination events are restricted to the acinar cell compartment, with apparent sparing of CACs. Nevertheless, as a second concurrent method to selectively activate mutant *Kras* in acinar cells, we incorporated the *Mist1*$^{Cre\text{ERT2}/+}$ model in our study. The *Mist1*$^{Cre\text{ERT2}/+}$ strain was generated by homologous recombination, replacing the entire *Mist1*-coding region with Cre-ERT2 cDNA. In wild-type mice, Mist1 protein is expressed in the nuclei of acinar cells, and is excluded from the Hes1-expressing CACs (see Supporting Information (SI) Fig. S1). Reciprocally, no Hes1 expression is seen in the acinar compartment. Conventional lineage tracing studies with *Mist1*$^{Cre\text{ERT2}/+}$; *Rosa26*R mice showed that most acinar cells and a few β cells were β-gal positive, while all duct cells remained convincingly negative (Fig. S2). However, this analysis did not convincingly exclude recombination occurring in individual CACs, due to the "bleeding" effect of strong acinar X-gal staining into the centro-acinar region. Therefore, we used a second lineage tracing experiment by generating bi-transgenic *Mist1*$^{Cre\text{ERT2}/+}$; CAG$_{\text{pr}}$-LSL-*Mist1*$^{\text{Myc}}$ mice, wherein tamoxifen administration results in *Cre*-activatable Mist1-Myc fusion protein expression within the *Mist1* domain. This experiment provided a level of sensitivity for distinguishing isolated CACs from surrounding acinar cells not afforded by conventional β-galactosidase staining in *Rosa26*R mice. The restricted nuclear expression of Myc and Hes1 antigens permitted the unequivocal delineation of acinar cells versus CACs, in both bright field and in fluorescence microscopy (Fig. S3). Thus, tamoxifen induction leads to robust Mist1-Myc fusion protein expression in the acinar cell compartment, while specifically excluding the individual Hes-1 expressing CACs. These results confirmed the essentially acinar-specific distribution of *Cre*-mediated recombination in the mature pancreas of *Mist1*$^{Cre\text{ERT2}/+}$ mice.

Lineage tracing and laser capture microdissection confirms that mPanIN lesions are acinar cell-derived progeny. We used two assays for confirming that *Cre*-mediated recombination had occurred

within the mPanIN lesions observed in both bi-transgenic models, as evidence supporting their acinar cell derivation. First, we generated *Mist1*$^{Cre\text{ERT2}/+}$; LSL-*Kras*^{G12D}; *Rosa*26R reporter mice, and harvested the pancreata of tamoxifen-induced mice at 2 months post-induction, which were then stained for β-galactosidase expression, as described (3, 9). The acinar compartment was expectedly stained in these mice, but so were the resulting mPanIN lesions, reinforcing a conserved lineage with acinar cells (Fig. S4*A* and *B*). In contrast, native ducts did not show β-galactosidase labeling, consistent with absence of recombination. We also microdissected five individual mPanIN lesions in the *Ela-Cre*ERT2$^{Tg/+}$; LSL- *Kras*^{G12D} mice (Figs. S4*C–E*), and confirmed recombination of the *lox*P sites in the mutant *Kras* allele, using a PCR strategy specifically designed to detect this recombination event (Fig. S4*F*). Expectedly, a band for the hemizygous wild-type allele was also detectable in this PCR.

Acinar cell-derived mPanINs are highly proliferative. The mPanIN lesions arising upon developmental *Kras*^{G12D} targeting in either the *Pdx1* or the *ptf1a*/*p48* expression domain are highly proliferative lesions (1, 11), analogous to their human counterparts (12). The mPanIN lesions arising in both tamoxifen-induced bi-transgenic models in the current study were also highly proliferative, as assessed by the diffuse nuclear expression of proliferating cell nuclear antigen (PCNA) (Figs. S5*A* and *B*) and Ki-67 (MIB-1) (Fig. S5*C*), respectively. Of interest, even lower histological grades of mPanIN were markedly proliferative, a feature also observed in low-grade mPanIN lesions occurring in the previously described *ptf1a*$^{Cre/+}$; LSL-*Kras*^{G12D} mice (11).

Targeting mutant Kras to the mature Pdx1 domain does not yield a pancreatic phenotype. The credentialed mouse models of PDAC have been generated via developmental activation of mutant *Kras* in the *Pdx1* expression domain. We sought to recapitulate these findings in the mature pancreas by generating bi-transgenic *Pdx1-Cre*ERT2$^{Tg/+}$; LSL- *Kras*^{G12D} mice. In the mature pancreas, high level *Pdx1* expression is restricted to the β cells, although extra-islet expression has been observed in the context of pancreatic injury and regeneration (13). Tamoxifen-induced recombination in the adult pancreas of *Pdx1-Cre*ERT2$^{Tg/+}$ mice has previously been observed to be restricted to β-cells within the islets, and to specifically be excluded in non-β islet cells, as well as in ductal and acinar cell populations (14). Unlike the striking pancreatic phenotype seen with acinar cell specific activation of *Kras*^{G12D}, no pancreatic lesions were observed in tamoxifen-induced *Pdx1-Cre*ERT2$^{Tg/+}$; LSL- *Kras*^{G12D} mice, which were followed up to 12 months postinduction (*data not shown*). Thus, the Pdx1-expressing cells in the mature pancreas appear to be relatively resistant to the oncogenic effects of mutant *Kras,* at least in the absence of additional genetic "hits" or exogenous injury.

1. Hingorani SR, *et al.* (2003) Preinvasive and invasive ductal pancreatic cancer and its early detection in the mouse. *Cancer Cell* 4:437–450.
2. Hingorani SR, *et al.* (2005) Trp53R172H and KrasG12D cooperate to promote chromosomal instability and widely metastatic pancreatic ductal adenocarcinoma in mice. *Cancer Cell* 7:469–483.
3. Fendrich V, *et al.* (2008) Hedgehog signaling is required for effective regeneration of exocrine pancreas. *Gastroenterology.*135:347–351.
4. Tuveson DA, *et al.* (2006) Mist1-KrasG12D knock-in mice develop mixed differentiation metastatic exocrine pancreatic carcinoma and hepatocellular carcinoma. *Cancer research* 66:242–247.
5. Del Monte G, Grego-Bessa J, Gonzalez-Rajal A, Bolos V, De La Pompa JL (2007) Monitoring Notch1 activity in development: evidence for a feedback regulatory loop. *Dev Dyn* 236:2594–2614.
6. Guerra C, *et al.* (2007) Chronic pancreatitis is essential for induction of pancreatic ductal adenocarcinoma by K-Ras oncogenes in adult mice. *Cancer Cell* 11:291–302.
7. Miyamoto Y, *et al.* (2003) Notch mediates TGF alpha-induced changes in epithelial differentiation during pancreatic tumorigenesis. *Cancer Cell* 3:565–576.
8. Stanger BZ, Dor Y (2006) Dissecting the cellular origins of pancreatic cancer. *Cell cycle* 5:43–46.
9. Desai BM, *et al.* (2007) Preexisting pancreatic acinar cells contribute to acinar cell, but not islet beta cell, regeneration. *J Clin Invest* 117:971–977.
10. Means AL, *et al.* (2005) Pancreatic epithelial plasticity mediated by acinar cell transdifferentiation and generation of nestin-positive intermediates. *Development* 132:3767–3776.
11. Zhu L, Shi G, Schmidt CM, Hruban RH, Konieczny SF (2007) Acinar cells contribute to the molecular heterogeneity of pancreatic intraepithelial neoplasia. *Am J Pathol* 171:263–273.
12. Maitra A, *et al.* (2003) Multicomponent analysis of the pancreatic adenocarcinoma progression model using a pancreatic intraepithelial neoplasia tissue microarray. *Mod Pathol* 16:902–912.
13. Jensen JN, *et al.* (2005) Recapitulation of elements of embryonic development in adult mouse pancreatic regeneration. *Gastroenterology* 128:728–741.
14. Gao N, *et al.* (2007) Foxa2 controls vesicle docking and insulin secretion in mature Beta cells. *Cell Metab* 6:267–279.

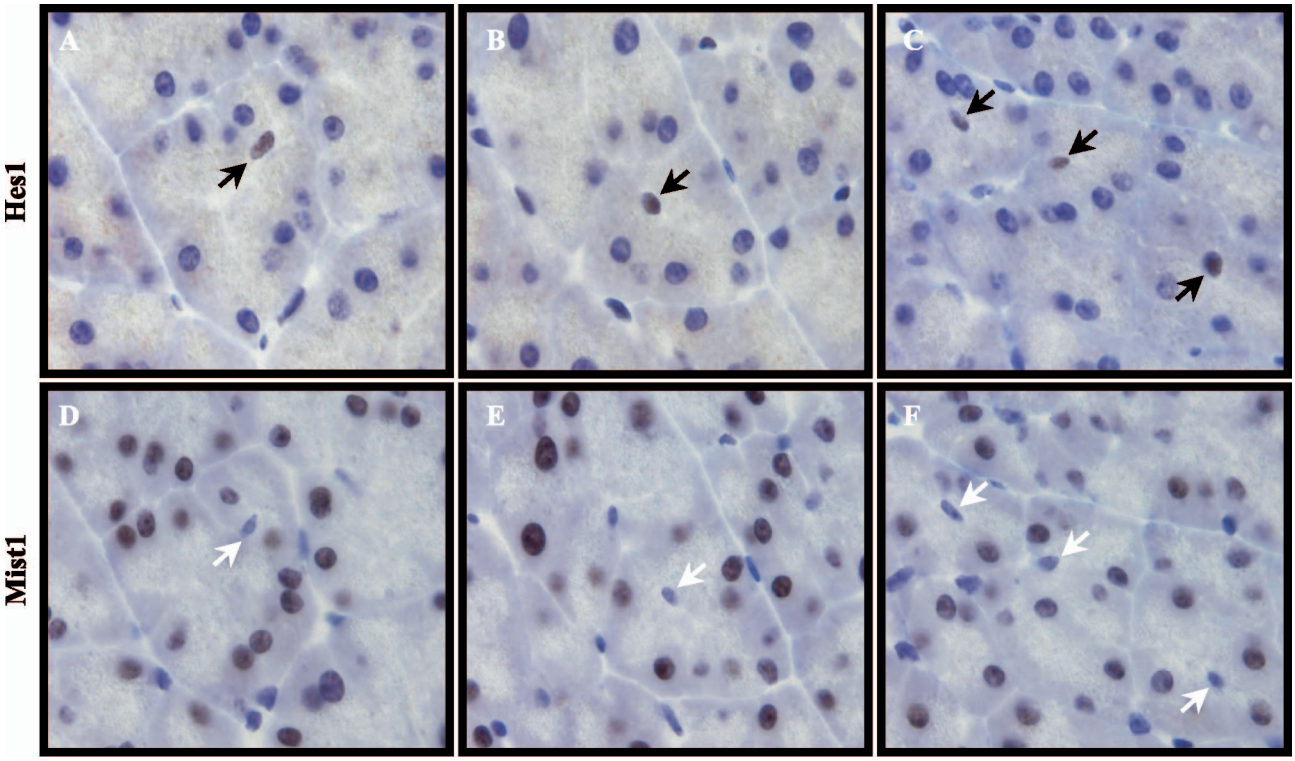

Fig. S1. Mist1 expression is restricted to the acinar compartment, and excludes centroacinar cells. (*A–C*) Multiple sections of pancreata from wild-type mice demonstrate nuclear Hes1 labeling in isolated centroacinar cells (CACs) (black arrows). The acinar compartment is Hes1 negative, as previously reported. (*D–F*) Serial sections from the pancreata illustrated above confirm that nuclear Mist1 is expressed in the acinar cells, but is specifically excluded from the CACs (white arrows).

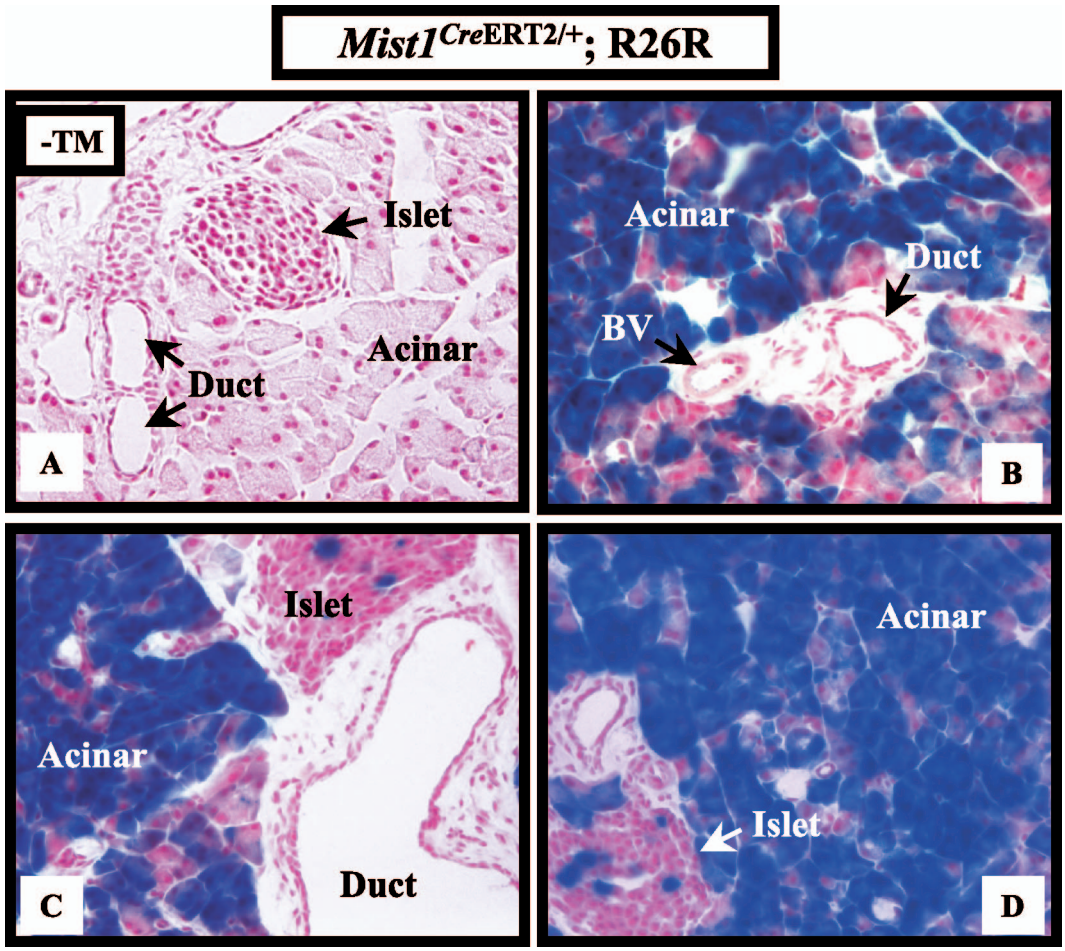

Fig. S2. Lineage tracing in ''knock-in'' *Mist1*$^{CreERT2/+}$; Rosa26R mice confirms recombination in acinar cells and occasional islet β cells. (*A*) Absence of discernible β-galactosidase expression in non-induced (-TM) *Mist1*$^{CreERT2/+}$; Rosa26R mice. (*B*) Uniform β-galactosidase expression in the acinar compartment of tamoxifen-induced *Mist1*$^{CreERT2/+}$; Rosa26R mice. In contrast, ductal epithelium and blood vessel (BV) in the photomicrograph are negative. (*C* and *D*) Additional examples of β-galactosidase expression in the acinar compartment of tamoxifen-induced *Mist1*$^{CreERT2/+}$; Rosa26R mice, and the absence of recombination in the ductal epithelium. Occasional β-cells in the islet also express β-galactosidase, consistent with Mist1 being expressed in these cells.

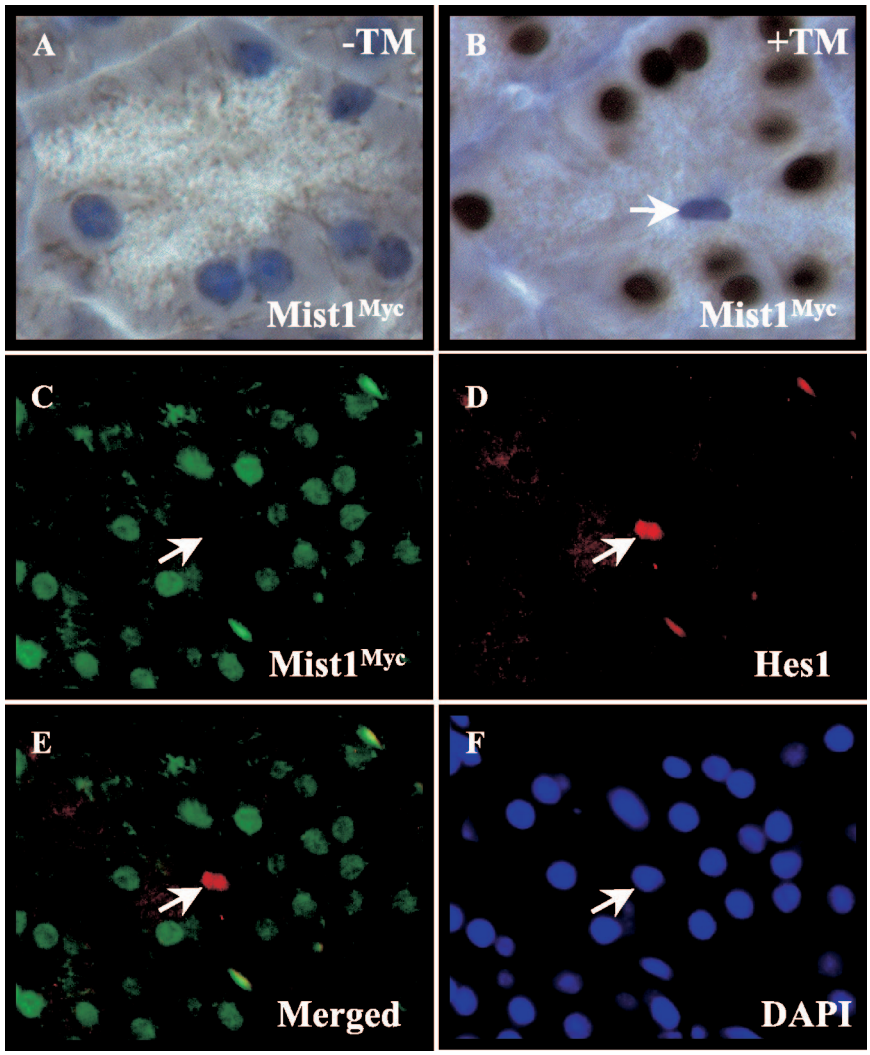

Fig. S3. Lineage tracing in *Mist1*$^{CreERT2/+}$; CAG_{pr}-LSL-*Mist1*^{Myc} mice confirms exclusion of Mist1 expression in CACs. (*A*) In the absence of tamoxifen induction (-TM), no Mist1-Myc fusion protein is expressed in the acinar cells of bi-transgenic mice. (*B*) Tamoxifen induction (+TM) results in diffuse nuclear expression of Mist1-Myc fusion protein (detected using anti-Myc antibody), while no labeling is seen in the nucleus of a CAC (white arrow). (*C–F*) Immunofluorescence studies on pancreata of tamoxifen induced *Mist1*$^{CreERT2/+}$; CAG_{pr}-LSL-*Mist1*^{Myc} mice confirm diffuse nuclear expression of Mist1-Myc fusion protein (anti-Myc1, green channel) in the nuclei of acinar cells, while no expression is observed in the Hes1-expressing CAC (anti-Hes1, red channel). DAPI (blue channel) is used as nuclear counterstain.

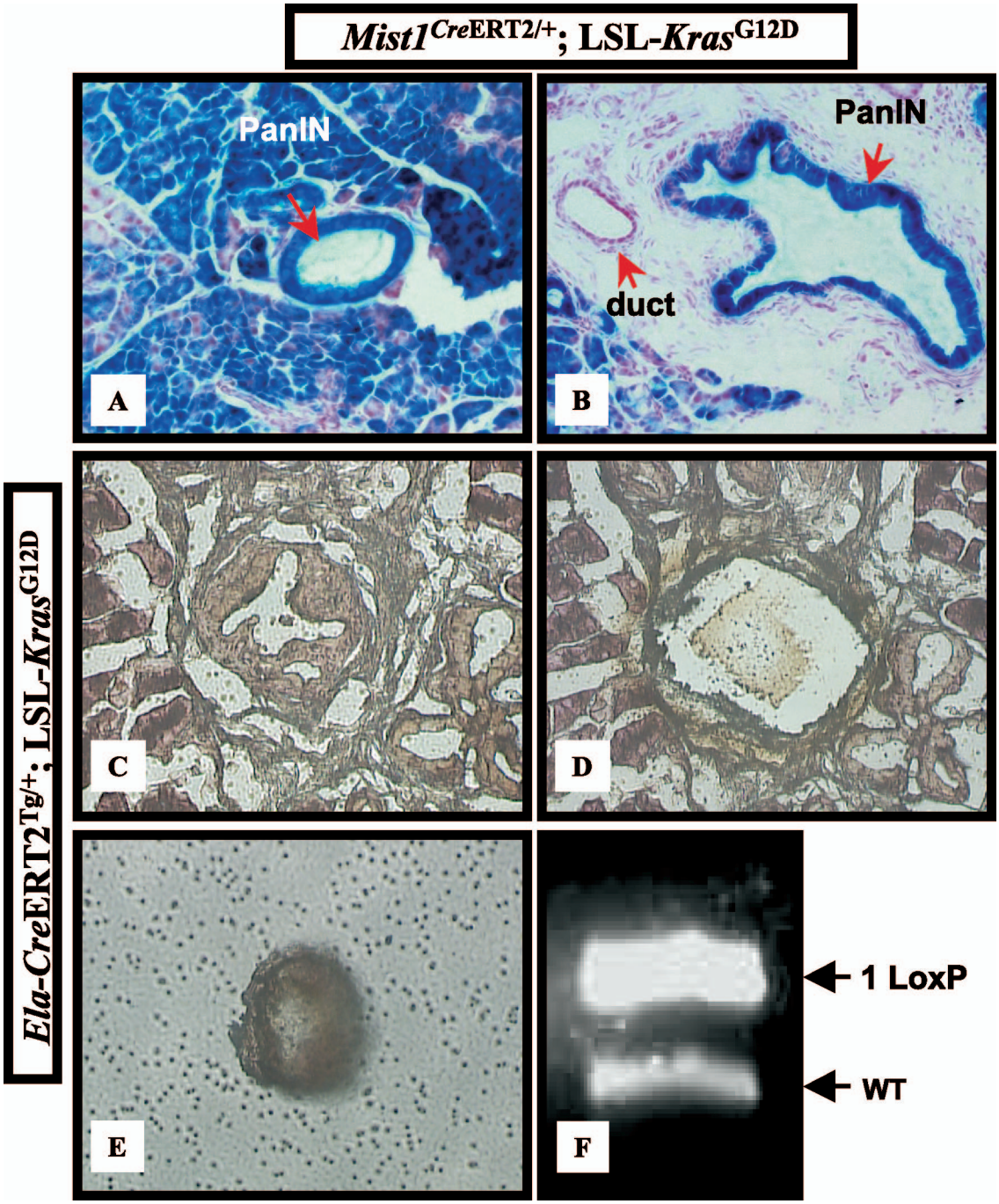

Fig. S4. Lineage tracing and PCR analyses of microdissected mPanIN lesions confirm acinar cell derivation. (*A*) Strong β-galactosidase expression in the acinar compartment and in the accompanying mPanIN lesion arising in a *Mist1*$^{CreERT2/+}$; LSL-*Kras*^{G12D}; *Rosa*26R reporter mouse. (*B*) An independent example of β-galactosidase expression in a mPanIN lesion arising in a *Mist1*$^{CreERT2/+}$; LSL-*Kras*^{G12D}; *Rosa*26R reporter mouse. In contrast, the adjacent native ductal epithelium does not demonstrate evidence of *Cre*-mediated recombination. (*C–E*) Microdissection of individual mPanIN lesions arising in *Ela-Cre*ERT2$^{Tg/+}$; LSL-*Kras*^{G12D} mice, using the PALM Laser MicroBeam platform. The illustrated example is a low-grade mPanIN of the type illustrated in Fig. 1. Note that adjacent acinar cells are left intact. See Fig. 4*C* for PCR experiments on microdissected mPanIN lesions. (*F*) PCR analysis of microdissected mPanIN lesion shows a strong band for the hemizygous *Kras*^{G12D} allele with one residual *lox*P site (''1loxP'', consistent with Cre-mediated recombination), and a second band for the remaining wild-type (''WT'') allele.

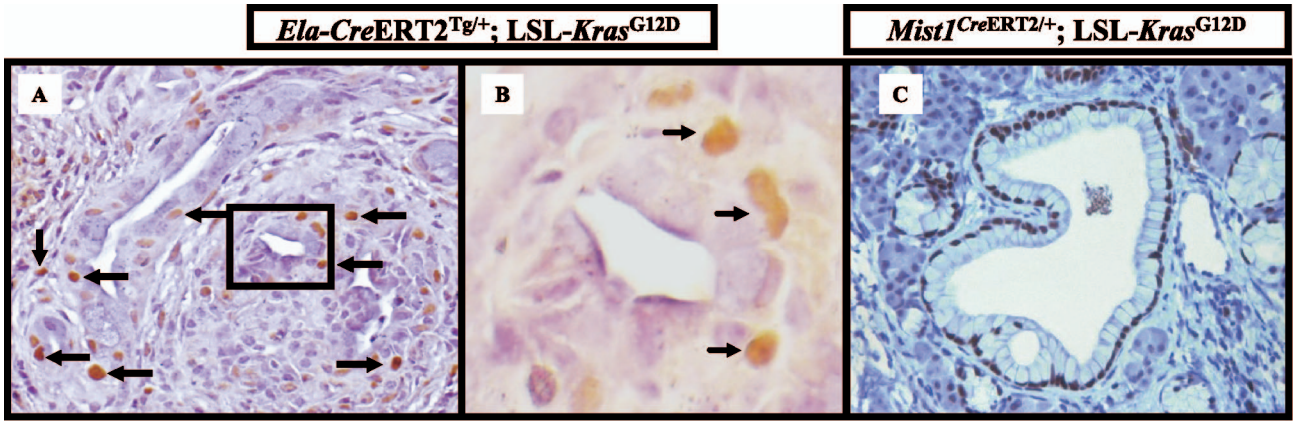

Fig. S5. Acinar cell-derived mPanIN lesions are highly proliferative. (*A*) Expression of proliferating cell nuclear antigen (PCNA) in mPanIN lesions arising in an *Ela-Cre*ERT2$^{Tg/+}$; LSL-*Kras*^{G12D} mouse, as assessed by immunohistochemistry (arrows). (*B*) High power view of the boxed region in (*A*) illustrating the nuclear expression of PCNA (arrows). (*C*) mPanIN lesions arising in *Mist1*$^{CreERT2/+}$; LSL-*Kras*^{G12D} mice are also highly proliferative, as assessed by expression of a different proliferation marker, Ki-67 (MIB-1), by immunohistochemistry.